

On the surface extraction of electrons in a pulsar

D. A. Diver, A. A. da Costa, E. W. Laing, C. R. Stark
and L. F. A. Teodoro

This article has been accepted for publication in Monthly Notices of the Royal Astronomical Society. © 2009 the authors. Journal compilation © RAS. Published by Oxford University Press on behalf of the Royal Astronomical Society. All rights reserved.

On the surface extraction of electrons in a pulsar

D. A. Diver,^{1*} A. A. da Costa,^{1,2} E. W. Laing,¹ C. R. Stark^{1,3} and L. F. A. Teodoro^{1†}

¹*Department of Physics and Astronomy, Kelvin Building, University of Glasgow, Glasgow G12 8QQ*

²*Secção de Telecomunicações, DEEC, Instituto Superior Técnico-UTL, 1049-001 Lisboa, Portugal*

³*School of Mathematics and Statistics, University of St Andrews, Mathematical Institute, St Andrews KY16 9SS*

Accepted 2009 September 8. Received 2009 August 13; in original form 2009 June 1

ABSTRACT

We present a novel description of how energetic electrons may be ejected from the pulsar interior into the atmosphere, based on the collective electrostatic oscillations of interior electrons confined to move parallel to the magnetic field. The size of the interior magnetic field influences the interior plasma frequency, via the associated matter density compression. The plasma oscillations occur close to the regions of maximum magnetic field curvature, that is close to the magnetic poles where the majority of magnetic flux emerges. Given that these oscillations have a density-dependent maximum amplitude before wavebreaking occurs, such waves can eject energetic electrons using only the self-field of the electron population in the interior. Moreover, photons emitted by electrons in the bulk of the oscillation can escape along the field lines by virtue of the lower opacity there (and the fact that they are emitted predominantly in this direction), leading to features in the spectra of pulsars.

Key words: acceleration of particles – plasmas – pulsars: general.

1 INTRODUCTION AND CONTEXT

The source of the plasma in pulsar magnetospheres is a subject that has long been at the heart of pulsar electrodynamics and is a problem still open to question (e.g. see review articles by Michel 1982, 2004). It is assumed that there must be an initial electron flux from the stellar surface and that these particles are then implicated in the production of the electron–positron plasma which populates the magnetosphere (Ruderman 1971; Sokolov & Ternov 1986; Harding & Lai 2006). The stellar surface in question is the transition between the pulsar interior and its atmosphere; the formation of an environmental pair plasma then must be linked to the energetics of electrons expelled from the outer crust into the atmosphere.

Therefore, we are interested primarily in the physical mechanism that extracts electrons from the interior, and projects them into the atmosphere immediately above the pulsar surface, where the electron–positron plasma is formed. This breaks down the fundamental pulsar problem into two parts.

- (i) From where do the energetic electrons come?
- (ii) Given these energetic electrons, what underlying physical processes cause the creation of the atmospheric pair-plasma?

This article attempts to contribute a new perspective on (i), the source and energetics of ejected electrons. The central idea is that

electrons are ejected from the magnetic flux tubes as a result of the self-field induced in plasma oscillations inside the tubes themselves, by virtue of the magnetic curvature. Electrons are assumed to be severely constrained to follow magnetic field lines in the interior; these lines are strongly curved near the poles, where the magnetic field emerges normal to the pulsar surface (this is because the magnetic field to some extent must run parallel to the curved surface in the interior, but then emerge in a small spot that constitutes the polar region; all emergent field lines are sharply refracted as they leave the iron crustal interior – a shell of iron surrounding a denser neutron core – and emerge into the atmosphere). The curvature of the field along which electrons are constrained to move causes density variations in the electron population, as particles are forced to lose parallel momentum. Such density variations cause electrostatic compressions and rarefactions of the electron ‘gas’ at the plasma frequency, with the self-electric-field providing the restoring force (i.e. the mutual repulsion of the negatively charged electrons).

These electrostatic waves also have a characteristic radiation signature at the plasma frequency, since the electrons are strongly accelerated when participating in this bulk motion. Given that regions of high magnetic flux have a relatively low opacity for photon transport, this means that photons radiated in this way are more likely to move parallel to the field and emerge at the pole. Given that the plasma density in the pulsar atmosphere is substantially less than that prevailing in the interior, the atmosphere is transparent to these photons, and we present tentative evidence that such signatures are already apparent in the X-ray spectra of selected objects.

The plasma frequency plays a key role here in the electrodynamics, and we show how the plasma frequency must be dependent on the magnetic field, since the latter causes the matter deformation

*E-mail: diver@astro.gla.ac.uk

†Present address: ELORET Corp., Space Sciences and Astrobiology Division, MS 254-3, NASA Ames Research Center, Moffett Field, CA 94935-1000, USA.

and compression that enables the perfectly conducting, anisotropic transport of electrons along flux tubes to exist.

The sections that follow address key issues in sequence: the magnetic compression and its influence over the plasma frequency; the dynamics of one-dimensional (1D) electrostatic waves and oscillations; the modelling of the Fermi energy and the associated maximum energy gain in an electron wave and a selection of possible candidate pulsars showing non-thermal features that correlate with the prediction of radiation at the internal plasma frequency. Concluding remarks finish the paper, and an explanatory Appendix gives more detail on the relativistic calculation of the Fermi energy.

2 DENSITY COMPRESSION AND THE PLASMA FREQUENCY

The process of extracting electrons from the outer crust requires the description of the structure of matter there, and this has to be supported with the study of the structure of atoms in strong magnetic fields.

There are various exotic descriptions of atoms in extreme magnetic fields, showing how the basic lattice structure of the conducting metal is severely distorted, with implications for the conduction electrons. Such models are controversial and, in some respects, difficult to reconcile [e.g. the literature (Neuhauser, Langanke & Koonin 1986; Neuhauser, Koonin & Langanke 1987; Lieb et al. 1992) is undecided about the complex nature of the bonding between iron atoms under such conditions].

However, the more general concept is widely accepted, namely that the magnetic compression of the atoms leads to an effective iron atomic radius R given by (Lai 2001)

$$R \approx Z^{1/5} b^{-2/5} a_0, \quad (1)$$

where Z is the atomic number (26 for Fe), $b = B/B_0$ is the ratio of the pulsar magnetic field to the critical field $B_0 = m_e^2 e^3 c / \hbar^3 = 2.35 \times 10^5$ T and $a_0 = 5.29 \times 10^{-11}$ m is the Bohr radius. For the typical pulsar field of 10^8 T, $b \approx 426$ and $R \approx 9 \times 10^{-12}$ m. The classical radius of Fe is $R_{\text{Fe}} = 1.4 \times 10^{-10}$ m (Slater 1964), so that the compression leads to an increase in matter density of $(R_{\text{Fe}}/R)^3 \approx 3.75 \times 10^3$. Of course, the free electron density is also increased as a direct consequence of this compression. Taking the free electron density of Fe under standard terrestrial conditions as $n_e^{\text{Fe}} = 1.7 \times 10^{29} \text{ m}^{-3}$ (Ashcroft & Mermin 1976), we can arrive at an electron number density for the pulsar n_e^{A} from atomic compression by applying the same scaling:

$$n_e^{\text{A}} \approx n_e^{\text{Fe}} \times 3.75 \times 10^3 \approx 6.4 \times 10^{32} \text{ m}^{-3} \quad (2)$$

which is a lower limit, since it is likely that there are more electrons able to access the conduction band under compression than in the classical limit.

However, there is another way of deriving the empirical electron number density in the pulsar crust. Iron has a monatomic body-centred cubic (BCC) crystal structure under standard terrestrial conditions, with inter-atomic spacing $a_{\text{Fe}} = 2.87 \times 10^{-10}$ m (Ashcroft & Mermin 1976). Assuming that the iron on the surface of the pulsar is also BCC (Ruderman 1971), this means that the compression factor here can be calculated in terms of the effective atom spacing in the pulsar environment compared with the terrestrial one.

The presence of extraordinarily large magnetic fields distorts the iron crystal from being isotropic to being severely anisotropic in transport terms: the iron is very highly conducting in the direction parallel to the magnetic field, but perpendicular transport is severely inhibited. The overall picture is of a set of perfectly conducting

‘tubes’ aligned locally with the ambient magnetic field direction along which electrons are able to move relatively freely; this description is qualitatively consistent with the ‘distorted atoms in a strong-field’ model. This is essentially the structure proposed by Ruderman (1971), Canuto & Ventura (1977) show that the conductivity parallel to the magnetic field is on average 20 times greater than that of the field-free case; conversely, the transverse conductivity has a strong dependence on the magnetic field and the Fermi energy, and is typically orders of magnitude smaller than the longitudinal case.

With this simple picture, we can capture the essence of the electron motion; parallel momentum is unconstrained, but perpendicular momentum is quantized. In Ruderman’s simple 1D flux tube (Ruderman 1971), the radius of the flux tube is set equal to the mean orbital radius associated with the Landau ground state:

$$\hat{\rho} = \left(\frac{\hbar}{eB} \right)^{1/2} \approx 2.6 \times 10^{-12} \text{ m}, \quad (3)$$

where we have taken $B = 10^8$ T.

In so doing, the simple 1D flux tube model assumes dominant parallel motion along the magnetic field, and assumes that the transport anisotropy is sufficient to render all non-trivial Landau levels as unimportant, effectively confining the electron to a single flux tube.

The scalelength $\hat{\rho}$ is then the effective inter-atom spacing in the compressed BCC structure, leading to a compression of $(a^{\text{Fe}}/\hat{\rho})^3 \approx 1.4 \times 10^6$ and an electron number density n_{eL} based on lattice compression of

$$n_e^{\text{L}} \approx n_e^{\text{Fe}} \times 1.4 \times 10^6 \approx 2.4 \times 10^{35} \text{ m}^{-3}. \quad (4)$$

Since we now have possible electron number densities ranging over more than two orders of magnitude, we shall take the geometric mean as the characteristic pulsar interior electron number density n_e :

$$n_e^{\text{A}} = n_e^{\text{Fe}} \chi_{\text{A}} b^{6/5} \approx 6.4 \times 10^{32} \text{ m}^{-3} \quad (5)$$

$$\chi_{\text{A}} = R_{\text{Fe}}^3 Z^{-3/5} a_0^{-3} \approx 2.61 \quad (6)$$

$$n_e^{\text{L}} = n_e^{\text{Fe}} \chi_{\text{L}} b^{3/2} \approx 2.4 \times 10^{35} \text{ m}^{-3} \quad (6)$$

$$\chi_{\text{L}} = a_{\text{Fe}}^3 (eB_0/\hbar)^{3/2} \approx 159 \quad (7)$$

$$\begin{aligned} n_e &= (n_e^{\text{A}} n_e^{\text{L}})^{1/2} = n_e^{\text{Fe}} (\chi_{\text{A}} \chi_{\text{L}})^{1/2} b^{1.35} \\ &\approx 3.5 \times 10^{30} \times b^{1.35} \text{ m}^{-3} \\ &\approx 1.23 \times 10^{34} \text{ m}^{-3}, \end{aligned} \quad (8)$$

where we have assumed a magnetic field of $B = 10^8$ T, that is $b \approx 426$.

The geometric mean compression yields a mass density of approximately 10^6 kg m^{-3} for ^{56}Fe , which is consistent with the conventional assumptions of density on the surface (Shapiro & Teukolsky 1983; Harding & Lai 2006).

The electron number density is a critical parameter for plasmas, since it defines the basic collective time-scale, namely the plasma frequency ω_p . Given that the interior is an excellent example of fixed positive ions and mobile electrons, we can define the plasma frequency here in terms of the electrons only:

$$\begin{aligned} \omega_p &= \left(\frac{n_e e^2}{\epsilon_0 m_e} \right)^{1/2} \\ &\approx 1.05 \times 10^{17} b^{0.675}, \end{aligned} \quad (9)$$

where we have used the geometric mean number density in the numerical evaluation; m_e and ϵ_0 are the electron rest mass and electric constant, respectively.

Note that the plasma frequency in the pulsar interior depends on the magnetic field strength; it is not an independent parameter. This is an important result that, although appearing to be a straightforward deduction from the mass density dependence well known in the literature, is still worth stressing because of the radiative consequences.

Having used a blend of the published equations of state for the bound material in the lattice to infer the free electron density, it is important to recognize that such free electrons are not required to obey the same equation of state as the bound matter: after all, the electrons in a cold plasma have no equation of state! Since the cold electron plasma is an excellent model for free electron behaviour in our pulsar interior, we shall therefore not require any further detailed analysis of the interior equation of state.

3 1D ELECTRON DYNAMICS

3.1 Calculating the Fermi energy

The simple assumption of such a strongly anisotropic conducting flux tube has major implications. The electron dynamics in the interior can be treated essentially as 1D, since the electron momentum parallel to the magnetic field greatly exceeds that perpendicular to it; hence in modelling the electron distributions, and deriving the Fermi energy as a substitute for the surface work function, a 1D treatment will be a good approximation. Moreover, since cross-field transport is inhibited, the role of the Landau levels in the interior is diminished: in the non-relativistic formulation of the electron motion in a uniform strong magnetic field B (Sokolov & Ternov 1986), the electron energy ϵ is given by

$$\epsilon \approx m_e c^2 + p_{\parallel}^2 / (2m_e) + \left(n + \frac{1}{2}\right) \hbar \omega_c, \quad (11)$$

where $\omega_c = eB/m_e$ is the cyclotron frequency, m_e is the electron rest mass and $n = 0, 1, 2, \dots$ is the principal quantum number for the quantized electron orbit in the plane perpendicular to the magnetic field. The radius R of orbit of the perpendicular motion of the electron can be expressed (in the same non-relativistic limit) as (Sokolov & Ternov 1986)

$$R = \left[\frac{2(n + \frac{1}{2}) \hbar}{eB} \right]^{1/2}. \quad (12)$$

The mean orbital radius associated with the Landau ground state is given by

$$R(n=0) = \left(\frac{\hbar}{eB} \right)^{1/2} \approx 2.6 \times 10^{-12} \text{ m}, \quad (13)$$

in other words $\hat{\rho} = R(n=0)$, in equation (3), as already assumed. Note that the energy increment $\delta\epsilon$ between Landau levels is

$$\delta\epsilon = \frac{\hbar e}{m_e} B \approx 10^{-4} B \text{ eV}, \quad (14)$$

where B is given in Tesla. Hence for a typical pulsar magnetic field of 10^8 T, Landau levels are separated by ~ 11.5 keV, implying that there is negligible population of the higher Landau levels if thermal excitation is the only mechanism, given that the typical surface temperature of a pulsar is $< 10^6$ K (in energetic terms, < 100 eV) (Bogdanov et al. 2006; Haberl 2007; Kargaltsev & Pavlov 2007).

This reinforces the merit in assuming that the electron momentum is largely parallel to the magnetic field and lends credence to the argument that a 1D statistical treatment captures the essential physics.

Finally, although calculations involving the Landau levels are quantum in nature, they are not relativistic (though the generalization is possible). For the moment, we will defer the detailed discussion about the need for a relativistic treatment to the Appendix.

In general, the distribution function for electrons in the presence of a magnetic field B is really the Fermi–Dirac distribution, f_{FD} ,

$$f_{\text{FD}} = \{\exp[(\epsilon \pm \mu_B B - \mu)/(k_B T)] + 1\}^{-1}, \quad (15)$$

where ϵ is the energy, μ is the chemical potential, μ_B is the magnetic moment of the electron and T is the temperature. In the limit $T \rightarrow 0$, $\mu \rightarrow \epsilon_F$, the Fermi energy, and since $\mu_B B \sim 6$ keV $\gg k_B T$ for $B \sim 10^8$ T, we can assume that the electrons are spin aligned in the lowest energy configuration, and so this term can be neglected. Hence we have

$$\begin{aligned} \lim_{T \rightarrow 0} f_{\text{FD}} &\simeq \lim_{T \rightarrow 0} \{\exp[(\epsilon - \mu)/(k_B T)] + 1\}^{-1} \\ &= \begin{cases} 1 & \text{for } \epsilon < \mu \\ 0 & \text{for } \epsilon > \mu \end{cases}. \end{aligned} \quad (16)$$

For temperatures such that $k_B T \ll \mu$, the distribution is therefore basically a step function, with all energy levels equally occupied up to μ , and none of the higher ones occupied.

Ruderman (1971) calculated the Fermi energy for the simple 1D case, motivated by the restricted motion of the electrons imposed by the enormous magnetic field strengths in the pulsar interior. The reason for calculating the Fermi energy is that ϵ_F is an excellent guide to the work function of the surface, i.e. the potential barrier which must be surmounted before interior particles can escape to the exterior.

Assuming that the mean electron energy is far below the Fermi temperature (so that the step-function nature of the Fermi distribution can be assumed), for N electrons in the population,

$$N = \int_0^{\infty} g(\epsilon) f_{\text{FD}}(\epsilon) d\epsilon \approx \int_0^{\mu} g(\epsilon) d\epsilon, \quad (17)$$

where $g(\epsilon)$ is the density of states for the electron gas, and $\mu = \epsilon_F$ is the Fermi energy in the limit of $T \ll T_F$. For the 1D electron gas, $g(k) dk = [L/(2\pi)] dk$, where L is the characteristic scalelength of the problem, and we have suppressed the normal degeneracy factor of 2, given the spin-alignment assumption. In this case, the integration yields

$$\epsilon_F = \frac{\hbar^2 N^2}{2m_e L^2}, \quad (18)$$

where we should interpret N/L as the line density of electrons. Assuming a uniform density approximation within the pulsar interior, the line density of electrons confined to a flux tube of radius $\hat{\rho}$ is simply the volume electron number density n_e times the cross-sectional area associated with the flux tube: $N/L = n_e \pi \hat{\rho}^2$. When substituted, this gives

$$\epsilon_F = \frac{\hbar^2 n_e^2 \pi^2 \hat{\rho}^4}{2m_e} = \frac{\hbar^4}{8m_e e^2} \frac{n_e^2}{B^2} \quad (19)$$

$$\begin{aligned} &\approx 1.03 \times 10^{-66} \frac{n_e^2}{B^2} \\ &\approx 2.28 \times 10^{-16} b^{0.7} \text{ J} \end{aligned} \quad (20)$$

in SI units. Equation (19) is essentially Ruderman's formula (Ruderman 1971).

Assuming a typical magnetic field of 10^8 T, and taking the electron number density from (8), yields

$$\epsilon_F \approx 97 \text{ keV}. \quad (21)$$

Note that the Fermi energy increases with magnetic field strength: this is because the electron number density increases faster than the field strength, no matter which scaling model is chosen. This is an important, if slightly counterintuitive, result, since the influence of the magnetic field in expressions for ϵ_F such as equation (19) suggest that an increasing magnetic field strength will lower the potential barrier at the poles. However, this neglects the indirect influence of B on the electron number density: increasing field strengths must lead to increased matter compression, and this must be taken into account in the Fermi-energy calculation.

Note that since the surface temperature of the pulsar T_p is below 10^6 K, equivalent in energy terms to <100 eV, then (21) is an acceptable approximation, since in this case it is self-evident that $T_p \ll T_F$.

The calculations presented here assume a 1D model for electron motion, and therefore preclude any contribution from Landau levels. The Appendix details the nature of the calculation where Landau levels must be included and where the energies are intrinsically relativistic.

3.2 Electron motion in inhomogeneous magnetic fields

The simple 1D description of the electron transport requires careful treatment when the magnetic field is not homogeneous. Magnetic field emerges from the interior predominantly at the poles; this concentration of the field lines at specific points on the surface means that there must be significant curvature inside (and outside) the star, as the field emerges from inside the iron spherical shell. Electrons constrained in the 1D model to follow these field lines are nevertheless inertial particles, and therefore cannot instantaneously change direction. However, they are also restricted in their perpendicular motion, since they have to satisfy the Landau quantization. In the simple 1D model, the electrons negotiate this magnetic field curvature in a non-quantal way, since scattering into Landau levels above the ground state is not permitted; therefore the electrons must change direction to follow the field direction, without any significant locally transverse excursions; momentum conservation must be provided by the crystal lattice, and the overall energy conservation must lead to electrons losing energy to the crystal as they negotiate the curve.

The overall effect of the magnetic inhomogeneity must be to introduce a local 'bunching' of electron density along the magnetic field direction in the region of greatest local curvature, i.e. near the magnetic poles. Note that complex magnetic geometries can be produced by thermal evolution of the neutron star itself (Page, Geppert & Küker 2004; Pons, Miralles & Geppert 2009), where strong toroidal field curvature can result from the strong magnetic feedback on thermodynamic transport properties. If strongly curved magnetic fields produced in such process lead to significant perpendicular field eruption at the pulsar surface, then these field lines will also act as electron ejection sources. A schematic of the situation is shown in Fig. 1. Such local density fluctuations will drive an electrostatic wave along the flux tube, accelerating (and decelerating) non-local electrons (ahead and behind the curved region) that populate this tube. Now either this is sufficient in itself to eject electrons at the end of the tube, where the surface exists, or the electrostatic

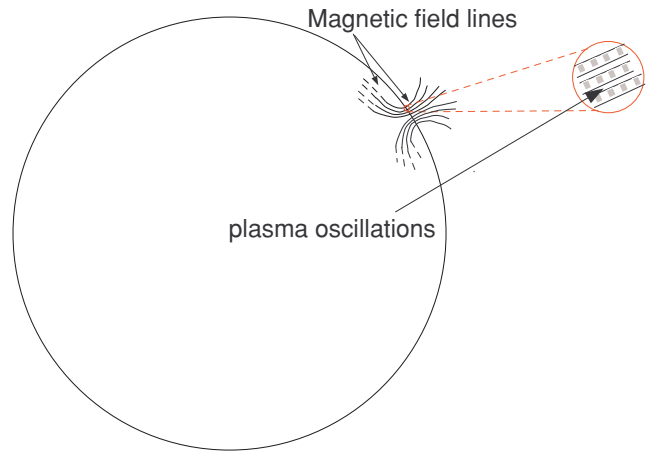


Figure 1. Schematic showing a simplified sketch of part of the magnetic field of the pulsar, interior and exterior (note that only a few magnetic field lines are included in order to keep the diagram simple). A small region near the pole is magnified to show the location of the electron oscillations induced by the curvature; the shaded regions are intended to illustrate density compressions. Note that strong magnetic field curvature can also be caused by magneto-convective processes not represented in this diagram.

wave itself evolves non-linearly and eventually breaks, leading to the ejection of a few relatively energetic particles ahead of the wave. Either way, it seems that such a description has the requisite element of a parallel acceleration mechanism that is self-consistent, and not dependent on any frame-transformed field component.

It is worth distinguishing between the electron temperature and the electron energy; mono-energetic beams of electrons are formally cold (i.e. possess zero temperature), yet can stream in the beam direction with significant energy. In the scenario outlined above, it is assumed that the mean energy of the electrons, including any directed streaming, is less than the Fermi energy, since otherwise a significant fraction of the interior electrons would simply leak out of the flux tube into the pulsar atmosphere at the surface. Whilst this might solve the electron production problem, there remains the issue of identifying the physical process that causes such streaming. For the purposes of this article, therefore, we will assume that the electrons are mostly trapped in the iron crust, just as the free electrons are trapped in a metal in a natural terrestrial context. As in the latter case, there needs to be a mechanism that provides the necessary energy for electrons to overcome the potential barrier at the interface between the pulsar surface and the vacuum (or atmosphere), before electrons can be liberated at the surface. Thermionic emission seems implausible, since the surface temperature is less than one-tenth of the Fermi temperature; hence our concentration on the (self-) electric field produced by charge concentrations of electrons in density waves.

On a more formal basis, electrons with energy less than the escape energy (i.e. the Fermi energy) that are directed towards the surface along the curving magnetic field lines must be reflected, since they cannot escape. Therefore, there must be two populations of electrons in motion along a flux tube: those that are moving towards the surface, and those that are moving towards the interior, having been reflected at some point. This is similar to the magnetic bottle effect (Boyd & Sanderson 2003) where charged particles are reflected at magnetic field concentrations; note that the analogy is not perfect, though, since in the magnetic bottle, particles are reflected simply because energy is transferred from parallel motion along the field to perpendicular motion in the form of Larmor orbits.

Such counterstreaming electrons will lead to density instabilities if the perturbations on each stream happen to evolve in phase such that they reinforce each other. The full dispersion relation for electrons moving parallel and antiparallel to the magnetic field direction with speed u is given by Boyd & Sanderson (2003):

$$\frac{\omega_1^2}{(\omega - ku)^2} + \frac{\omega_2^2}{(\omega + ku)^2} = 1 \quad (22)$$

in which $\omega_i^2 = n_i e^2 / (\epsilon_0 m_e)$ is the square of the plasma frequency for electrons moving parallel to the magnetic field with speed u , where n_i is the number density of such electrons; ω_2^2 is similarly defined for electrons moving antiparallel to the field. We have assumed symmetry in the modelling, for simplicity; clearly we expect $n_1 \approx n_2$, which is equivalent to saying that the electron loss rate is small; hence we also expect $\omega_i \approx \omega_p, i = 1, 2$. The frequency and wavenumber of the common perturbation on the electron streams are given by ω and k , respectively. We must solve equation (22) in order to arrive at the criteria for instability. Manipulation of the algebra reveals that the dispersion relation is biquadratic in ω and that there are imaginary components of frequency (or wavenumber) when $u < \sqrt{2}\omega_p/k$. Put another way, any density perturbations with a wavelength λ satisfying

$$\frac{2\pi u}{\sqrt{2}\omega_p} < \lambda < R_* \quad (23)$$

must be unstable, where we have taken the upper limit on the wavelength to be the maximum scalelength in the star itself, that is, the pulsar radius R_* . Since the lower limit is at most $2\pi c / (\sqrt{2}\omega_p) \approx 5 \times 10^{-10} \text{ m} \approx 200\hat{\rho} \ll R_*$, then it is always possible for instabilities to affect the counterstreaming flows, in the form of longitudinal plasma oscillations at the plasma frequency.

There are further assumptions in this simple treatment, namely that the plasma density is uniform and the electrons are monoenergetic. These assumptions are fine in the context of an idealized cold plasma treatment; we contend that they serve as an adequate illustration in the context of the pulsar flux tube.

The nature of this streaming instability is to induce electrostatic oscillations on the dynamic electron population inside the flux tube.

These plasma oscillations produce a self-electric-field because of the compression and rarefaction of electron density; there is no associated magnetic perturbation, since the particle and displacement currents cancel perfectly. Note that this is a pure electron plasma with a fixed positive ion background, and so density enhancements here are pure electron overdensities. There is however a maximum amplitude of electric field associated with such oscillations. If the wavenumber is k , then in the non-relativistic limit, this maximum electric field E_{max} (Kruer 1990; Mori & Katsouleas 1990):

$$E_{\text{max}} = \frac{m_e \omega_p^2}{ek} \quad (24)$$

This result can be extended to the relativistic case:

$$E_{\text{max}} = \sqrt{2} \frac{\omega_p m_e c}{e} (\gamma_\phi - 1)^{1/2}, \quad (25)$$

where $\gamma_\phi = (1 + p_\phi^2 / (m^2 c^2))^{1/2}$ is the relativistic factor for maximum associated electron momentum p_ϕ in the oscillation. This is the limiting field before coherent motion breaks down and wave-breaking occurs, at which point part of the electron population begins free streaming at speeds greater than the phase velocity of the oscillation itself (Kruer 1990; Mori & Katsouleas 1990).

Consider the case of an electrostatic oscillation in a flux tube, very close to the surface near the magnetic pole. If the oscillation is at the point of wavebreaking, then the maximum energy $\delta\epsilon$ that

can be gained by an electron falling through the self-field of the oscillation before free streaming must be given by

$$\begin{aligned} \delta\epsilon &\approx e E_{\text{max}} \times \text{distance travelled by electron} \\ &\approx e E_{\text{max}} \pi / k. \end{aligned}$$

This electron will escape to the surface if it has an energy greater than the Fermi energy. Hence for escaping electrons,

$$e E_{\text{max}} \pi / k > \epsilon_F \quad (26)$$

which can be expressed as

$$k^2 < \frac{\pi m_e \omega_p^2}{\epsilon_F} \approx 5.6 \times 10^{20} b^{0.65} \text{ m}^{-2}, \quad (27)$$

using equations (4), (10) and (20). For the typical pulsar magnetic field, $b \approx 426$, yielding $k < 1.7 \times 10^{11} \text{ m}^{-1}$. In other words, plasma oscillations with wavelengths (or scale variations) $\lambda = 2\pi/k$ exceeding $4 \times 10^{-11} \text{ m}$ can eject electrons from the surface, providing such oscillations are at maximum amplitude. This minimum wavelength is considerably greater than $\hat{\rho} \approx 2.6 \times 10^{-12}$, the width of the flux tube (and the effective inter-ion spacing), suggesting that whilst the breakdown of ultra-short wavelength oscillations cannot provide sufficient energy for electrons to escape the surface, longer wavelength oscillations will readily do so.

Thus, we have shown that instabilities in the electron dynamics within the flux tube are sufficient to eject electrons from the pulsar interior.

Given that the opacity of the pulsar to photons of frequency ω is reduced by a factor of $(\omega/\omega_c)^2$ for propagation parallel to the magnetic field direction (Canuto 1975; Lai 2001), where $\omega_c = eB/m$ is the electron cyclotron frequency, there is the enhanced prospect of photons characteristic of the oscillation within the flux tube escaping directly to the pulsar atmosphere; in this context, $\omega = \omega_p$, and $(\omega_p/\omega_c)^2 \approx 6.4b^{-0.65} \approx 0.12$ for magnetic fields of 10^8 T , leading to the enhanced probability that the magnetic polar regions are transparent to the emission of keV photons (from the plasma oscillation) produced inside the flux tubes by the bulk plasma dynamics. Note that for magnetic fields of around $4 \times 10^6 \text{ T}$, this opacity enhancement disappears, and so direct emission of photons below 0.4 keV by this process would not be expected.

There has been considerable discussion of the electromagnetic transmission properties of the pulsar crust, particularly in the strong-field limit relevant to magnetars, in which the free electrons in the crust influence the transmission of the blackbody radiation from the pulsar surface itself (see e.g. Turolla, Zane & Drake 2004; van Adelsberg et al. 2005; van Adelsberg & Lai 2006). Strictly, this article presents a discussion of the electrostatic (not electromagnetic) behaviour of electrons oscillating at the interior plasma frequency. These electrons radiate in the local oscillating electric fields close to the surface such that some of the radiated photons escape from the interior and are able to propagate in the pulsar environment; a fraction of them may survive atmospheric processes to reach the observer. It is therefore helpful to clarify that the characteristic non-thermal signature of such a process as described in this article is not affected by the cold plasma twin-mode electromagnetic absorption properties of the crust as discussed in the literature.

Of course, the picture is further complicated by the fact that the self-field of the oscillation can accelerate particles in the perpendicular direction (MacLachlan, Diver & Potts 2009). Whilst the 1D model forbids perpendicular transport within the flux tube inside the pulsar, this restriction is no longer valid at the transition to the atmosphere (since the confining crystal lattice is no longer imposing dynamical constraints), and it is possible that some of the emitted

electrons will possess a perpendicular velocity component relative to the magnetic field direction very close to the surface, leading to a spread in exit trajectories for escaping electrons.

4 SUPPORTING FEATURES IN NEUTRON STAR X-RAY SPECTRA

We offer the following examples from *XMM-Newton* observations in support of our hypothesis that there is non-thermal radiation at the internal plasma frequency present in the pulsar emissions. The motivation for searching for such a non-thermal signature in X-ray spectra is that its presence in an object's spectrum lends plausibility to the electron production process actually occurring in that object.

It is established in the literature that X-ray pulsars commonly have a significant soft X-ray excess (Hickox, Narayan & Kallman 2004), but not all such excess signals come from accretion processes (see e.g. points 3–5 in the conclusions of Hickox et al. 2004). We offer here some examples in which we suggest that certain X-ray spectral features can be associated with the novel physical processes described in this article. Sifting all available data in support of non-thermal emission that could be attributed to plasma frequency radiation from the poles is a daunting task, not just because such signals are magnetic field and geometry dependent, and may in fact lie outside the spectral range for *XMM-Newton*. However, we did find several examples, which are described below. The magnetic field strengths in each example (other than in the case of De Luca et al. 2004) were taken from the Ioffe pulsar catalogue.¹

Please note that the predicted plasma frequencies are pulsar surface values; terrestrial observation of such features will incur a gravitational redshift of up to 25 per cent.

De Luca and co-workers (De Luca et al. 2004) showed detailed observations of the X-ray spectrum of the neutron star 1E 1207.4-5209, principally to demonstrate the presence of cyclotron absorption features at 0.7, 1.4, 2.1 and 2.8 keV, from which a surface magnetic field strength of $B \approx 6 \times 10^6$ T was derived, significantly different from the field of 2.6×10^8 T derived conventionally from timing parameters. The interpretation of the higher harmonics has been challenged (Mori, Chonko & Hailey 2005) as an instrumental effect. However, assuming that the lower magnetic field strength is correct, and using the plasma frequency given by equation (10) for this field strength, we calculate $\omega_p \approx 9.4 \times 10^{17}$ rad s⁻¹, generating photons with energy $h\nu_p$ of approximately 0.62 keV. This is very close to an excess above blackbody radiation in the phase integrated emission in the band 0.1–2.5 keV, just before the absorption feature at 0.7 keV (see fig. 6 in De Luca et al. 2004). Caution must be exercised here, since there is also a sharp drop in the CCD efficiencies in both the PN and MOS1 instruments at 0.5 eV (Kirsch 2004); however, since the observations show a rise above the blackbody spectrum before 5 eV, followed by a sharp drop, it is reasonable to assume that the excess is genuinely observed.

PSR J0538+2817 (McGowan et al. 2003; Zavlin & Pavlov 2004) has a surface magnetic field strength of 7.33×10^7 T, giving $h\nu_p \approx 3.3$ keV. The energy spectrum of this pulsar shows a marked excess over the blackbody emission at 3 keV (see fig. 4 in McGowan et al. 2003) consistent with non-thermal emission from the pole via the mechanism reported here. There are no calibration issues at these energies with the PN and MOS1 instruments on *XMM-Newton*, both of which recorded the excess signal.

The surface magnetic field of Geminga (Zavlin & Pavlov 2004) is 2×10^8 T, implying that radiation from the subsurface plasma oscillation will be at energies ~ 6.6 keV. The fitted European Photo Imaging Camera count-rate spectrum shows a clear departure from the model blackbody spectrum in the range 6–8 keV, as shown in fig. 6 of Zavlin & Pavlov (2004).

PSR J1932+1059 (B1929+10) shows a small feature at 2 keV (Wozna, Kuiper & Hermsen 2003, fig. 4) which is not fitted by either the blackbody spectrum or the power law. The pulsar has a surface field of $B_s = 5.18 \times 10^7$ T, suggesting that the plasma frequency yields photons of around 2.6 keV, offering a plausible explanation of this spectral feature.

If the identified spectral features are associated with the plasma frequency, then this means that there are indeed plasma oscillations present at the poles, and therefore it is also possible that such oscillations are contributing to the production of high-energy electrons in the atmosphere. Whilst it is arguable that the features we are citing here are close to being borderline in terms of statistical significance, we contend, nevertheless, that they offer a tantalizing glimpse of what might be the seat of the electron expulsion mechanism, and, as such, merit attention.

5 CONCLUDING DISCUSSION

The general scenario presented in this paper is as follows. Plasma oscillations are induced in the throat of the tightly curving magnetic field structure as it exits the pulsar interior at the magnetic poles. Such oscillations can sustain maximum amplitude electric fields such that at wavebreaking, electrons can be accelerated to energies in excess of the Fermi energy and ejected from the interior into the immediate pulsar environment. This behaviour could be intermittent, since the transit time for electrons to move along a magnetic field line from one pole to the other is less than a typical pulsar period (less than an ms, in fact), and so there could be an influence on the subpulse structure.

In addition to ejecting energetic electrons, the accelerations associated with these interior plasma oscillations will give rise to radiated photons which escape along the low-opacity field lines and emerge at the magnetic poles. Since the electron density immediately above the magnetic pole (produced by the ejection of electrons from a lossy mirror) is much less than that in the interior, any plasma oscillation radiation that leaks out will propagate away – photons of around 10^{17} Hz (around 2 keV) could be directly emitted from the polar region by interior oscillations – another source of moderate energy radiation. We have presented evidence of X-ray spectra of pulsars which show behaviour of this kind.

Given that the self-field in the interior of the flux tube is the source of the acceleration, this field will not be uniformly aligned with the magnetic field, leading to the possibility of highly energetic imperfectly aligned electrons very close to the pulsar surface. Such electrons could gyrorotate (subject to Landau levels) and radiate, or perhaps even collide with iron nuclei; either way, energetic photons are possible directly from the surface.

Of course, the pulsar still loses electrons this way; charge balance must be maintained ultimately, and this is probably achieved by a combination of sucking in electrons from the electron cloud above the poles (each half-cycle the self-field of the oscillation will reverse) and surface diffusion of electrons back into the interior from the exterior. Note that any positive potential arising from electron depletion of the pulsar will increase the work function (as distinct from the Fermi energy), making the potential barrier higher for electrons to escape the surface. It is conceivable that such charging

¹ <http://www.ioffe.ru/astro/1/psr-catalog/Catalog.php>

considerations could be sufficient to suppress electron ejection at the surface, even to the point of influencing the pair production in the atmosphere.

This general picture has several favourable aspects: not only does it provide a plausible source of parallel acceleration, leading to electron production at the magnetic poles, but also there is the real possibility of producing azimuthal structure in the electron production at the surface, arising from the mutual interaction of waves in adjacent flux tubes. Moreover, this model is consistent with the ideas associated with the distortion of atoms under strong magnetic fields giving rise to sheaths of free electrons aligned with those fields; it also yields accelerating parallel electric fields, albeit from a different physical process.

It is also worth noting that dropping the magnetic field strength raises the Fermi energy at the surface (since the strong field is suppressing the work function); this in turn reduces the spectrum of electrostatic oscillations that can eject free electrons, reducing the efficiency of atmospheric electron production and the associated energetic beaming processes. This may give an insight into transient pulsar behaviour, for those objects with weaker surface fields.

ACKNOWLEDGMENTS

DAD gratefully acknowledges funding from the UK Science and Technology Funding Council (STFC/F002149/I), as does CRS (PP/E001122/1). AADC is grateful to the Fundação para a Ciência e Tecnologia, Portugal, under Grant SFRH/BSAB/771/2007, who sponsored his sabbatical leave; thanks are due equally to the Instituto Superior Técnico and to the Department of Physics and Astronomy, University of Glasgow, for respectively granting and hosting AADC's sabbatical leave. LFAT is grateful to the Leverhulme trust for funding at Glasgow University. Finally, thanks are due to H.E. Potts, C.S. MacLachlan and E. Bennet for their helpful comments and stimulating discussion. The Department of Physics and Astronomy in the University of Glasgow is a member of the Scottish Universities Physics Alliance. We are also grateful to the anonymous referee, whose valuable feedback helped us improve this article.

REFERENCES

- Ashcroft N. W., Mermin N. D., 1976, *Solid State Physics*. Holt, Rinehart & Winston, New York
- Bogdanov S., Grindlay J. E., Heinke C. O., Camilo F., Freire P. C. C., Becker W., 2006, *ApJ*, 646, 1104
- Boyd T. J. M., Sanderson J. J., 2003, *The Physics of Plasmas*. Cambridge Univ. Press, Cambridge
- Canuto V., 1975, *Ann. New York Acad. Sci.*, 257, 108
- Canuto V., Ventura J., 1977, *Fundamentals Cosmic Phys.*, 2, 203
- De Luca A., Mereghetti S., Caraveo P. A., Moroni M., Mignani R. P., Bignami G. F., 2004, *A&A*, 418, 625
- Haberl F., 2007, *Ap&SS*, 308, 181
- Harding A. K., Lai D., 2006, *Rep. Prog. Phys.*, 69, 2631
- Hickox R. C., Narayan R., Kallman T. R., 2004, *ApJ*, 614, 881
- Kargaltsev O., Pavlov G., 2007, *Ap&SS*, 308, 287
- Kirsch M., 2004, *XMM-Newton Epic Status of Calibration and Data Analysis*. <http://xmm.vilspa.esa.es/docs/documents/CAL-TN-0018-2-3.pdf>, Garching (ESA)
- Kruer W. L., 1990, *Phys. Scr.*, T30, 5
- Lai D., 2001, *Rev. Mod. Phys.*, 73, 629
- Lieb E. H., Solovej J. P., Yngvason J., 1992, *Phys. Rev. Lett.*, 69, 749
- McGowan K. E., Kennea J. A., Zane S., Córdova F. A., Cropper M., Ho C., Sasseen T., Vestrand W. T., 2003, *ApJ*, 591, 380

- MacLachlan C. S., Diver D. A., Potts H. E., 2009, *New J. Phys.*, 11, 063001
- Michel F. C., 1982, *Rev. Mod. Phys.*, 54, 1
- Michel F. C., 2004, *Adv. Space Res.*, 33, 542
- Mori W. B., Katsouleas T., 1990, *Phys. Scr.*, T30, 127
- Mori K., Chonko J. C., Hailey C. J., 2005, *ApJ*, 631, 1082
- Neuhauser D., Langanke K., Koonin S. E., 1986, *Phys. Rev. A*, 33, 2084
- Neuhauser D., Koonin S. E., Langanke K., 1987, *Phys. Rev. A*, 36, 4163
- Page D., Geppert U., Küker M., 2007, *Ap&SS*, 308, 403
- Pons J. A., Miralles J. A., Geppert U., 2009, *A&A*, 496, 207
- Ruderman M., 1971, *Phys. Rev. Lett.*, 27, 1306
- Shapiro S. L., Teukolsky S. A., 1983, *Black Holes, White Dwarfs and Neutron Stars*. John Wiley & Sons, New York
- Slater J. C., 1964, *J. Phys. Chem.*, 41, 3199
- Sokolov A. A., Ternov I. M., 1986, *Radiation from Relativistic Electrons*, AIP Translation Series. Am. Inst. Phys., New York
- Turolla R., Zane S., Drake J. J., 2004, *ApJ*, 603, 265
- van Adelsberg M., Lai D., 2006, *MNRAS*, 373, 1495
- van Adelsberg M., Lai D., Potekhin A. Y., Arras P., 2005, *ApJ*, 628, 902
- Wozna A., Kuiper L., Hermsen W., 2003, in Cusumano G., Massaro E., Mineo T., eds, *Proc. Intl. Workshop, Marsala, Pulsars, AXPs and SGRs Observed with BeppoSAX and Other Observatories*, preprint (astro-ph/0302452)
- Zavlin V. E., Pavlov G. G., 2004, *Mem. Soc. Astron. Ital.*, 75, 458

APPENDIX A:

A1 Calculation of Fermi energy in a Landau levels environment

The general case should take into account the effect of Landau levels on the Fermi energy. In fact, the Fermi energy is dependent on the linear density of the electrons along the magnetic induction field lines, and the regime becomes relativistic above certain values. Following this idea, the energy $\epsilon = \gamma mc^2$ is given by

$$\gamma = \begin{cases} \sqrt{1 + \frac{p_{\parallel}^2}{m^2 c^2} + 2n\hbar \frac{eB}{m^2 c^2}} & \text{spin up} \\ \sqrt{1 + \frac{p_{\parallel}^2}{m^2 c^2} + 2(n+1)\hbar \frac{eB}{m^2 c^2}} & \text{spin down.} \end{cases} \quad (\text{A1})$$

Then, we see that the same value of γ has two possible values (n and $n+1$) with the exception $n=0$. Then the total number of electrons is given by

$$N = \frac{L}{2\pi\hbar} \sum_n \int \frac{dp_{\parallel}}{\exp\left[\frac{\epsilon(n, p_{\parallel}) - \mu}{kT}\right] + 1} \quad (\text{A2})$$

because the transverse moment is filled in Landau levels.

The value of the Fermi energy is $\epsilon_F = \lim_{T \rightarrow 0} \mu$, and therefore (16) implies, using $p_{\parallel} = \varpi_{\parallel} mc^2$, that there are upper limits for n and ϖ_z . Putting $\epsilon = \epsilon - mc^2 = \epsilon_1 mc^2$ and $\mu = \mu_1 mc^2$, $\kappa = \hbar\omega/mc^2$ with

$$\epsilon_1 = \sqrt{1 + \varpi_{\parallel}^2 + n\kappa} - 1. \quad (\text{A3})$$

The upper limits of ϖ_{\parallel} are reached when $\mu_1 = \epsilon_1$, and therefore the limits of integration are

$$\varpi_{\parallel} = \begin{cases} \sqrt{\mu_1^2 + 2\mu - 2n\kappa} & \text{spin up} \\ \sqrt{\mu_1^2 + 2\mu - 2(n+1)\kappa} & \text{spin down} \end{cases} \quad (\text{A4})$$

$$n \in \left[0, \text{int} \left(\frac{\mu_1^2 + 2\mu_1}{\kappa} \right) \right]. \quad (\text{A5})$$

After some algebra we find that

$$\frac{N}{L} \frac{h}{mc} = \sum_0^{\text{int}[(\mu_1^2 + 2\mu_1)/\kappa]} [\sqrt{\mu_1^2 + 2\mu_1 - n\kappa} \quad (\text{A6})$$

$$+ \sqrt{\mu_1^2 + 2\mu_1 - (n+1)\kappa} \quad (\text{A7})$$

an equation in μ_1 whose solution has to be found numerically, provided

$$\frac{\mu_1^2 + 2\mu_1}{\kappa} > 1. \quad (\text{A8})$$

However, if only $n = 0$ is present, this equation turns into

$$\frac{N}{L} \frac{h}{mc} = \sqrt{\mu_1^2 + 2\mu_1} + \sqrt{\mu_1^2 + 2\mu_1 - \kappa} \quad (\text{A9})$$

with general solution

$$\mu_1 = -1 + \left[1 + \left(\frac{N}{2L} \frac{h}{mc} + \kappa \frac{L}{2N} \frac{mc}{h} \right)^2 \right]^{1/2}. \quad (\text{A10})$$

If $(\frac{N}{2L} \frac{h}{mc} + \kappa \frac{L}{2N} \frac{mc}{h})^2 \ll 1$, then equation (A10) reduces to

$$\mu_1 \approx \frac{1}{2} \left(\frac{N}{2L} \frac{h}{mc} + \kappa \frac{L}{2N} \frac{mc}{h} \right)^2 \quad (\text{A11})$$

whereas in the limit $(\frac{N}{2L} \frac{h}{mc} + \kappa \frac{L}{2N} \frac{mc}{h})^2 \gg 1$

$$\mu_1 \approx \frac{N}{2L} \frac{h}{mc} + \kappa \frac{L}{2N} \frac{mc}{h}. \quad (\text{A12})$$

Equation (A11) is similar to Ruderman's (Ruderman 1971) expression for the Fermi energy when we neglect the spin effects and the zero-order energy. This means it can only be applied to sub-relativistic regimes. However, the general solution equation (A10) also contains the relativistic case for high-density electrons or large magnetic field amplitudes.

The overall solution shows that the value of the Fermi energy depends on the value of the magnetic field, and if

$$\left(\frac{N}{2L} \frac{h}{mc} \right)^2 < \frac{\hbar e B}{m^2 c^2}, \quad (\text{A13})$$

it may even be the dominant term determining its value. However, for the particular case of exclusively longitudinal motion, there should not be any dependence on the magnetic field; that it enters the Fermi energy even in this case is puzzling.

Moreover, the combination of a quantum statistical description in the perpendicular plane and a classical one along the magnetic field leads to the situation in which the statistics may preclude occupation of any Landau levels other than the zero one, as given in equation (A8). These contradictions between the description in Landau Levels and the underlying statistics have to be resolved in future.

This paper has been typeset from a $\text{\TeX}/\text{\LaTeX}$ file prepared by the author.